Check for updates

THE AMERICAN SOCIETY OF MECHANICAL ENGINEERS
Three Park Avenue, New York, N.Y. 10016-5990

99-GT-424

The Society shall not be responsible for statements or opinions advanced in papers or discussion at meetings of the Society or of its Divisions or Sections, or printed in its publications. Discussion is printed only if the paper is published in an ASME Journal. Authorization to photocopy for internal or personal use is granted to libraries and other users registered with the Copyright Clearance Center (CCC) provided $3/article is paid to CCC, 222 Rosewood Dr., Danvers, MA 01923. Requests for special permission or bulk reproduction should be addressed to the ASME Technical Publishing Department.

Copyright © 1999 by ASME All Rights Reserved Printed in U.S.A.

DETAILED MASS TRANSFER DISTRIBUTION IN ROTATING, TWO-PASS RIBBED COOLANT CHANNELS WITH VORTEX GENERATORS

by

V. Eliades, D. E. Nikitopoulos and S. Acharya[1]
Mechanical Engineering Department
Louisiana State University
Baton Rouge, LA 70803

Downloaded from http://asmedigitalcollection.asme.org/GT/proceedings-pdf/GT1999/78606/V003T01A096/2412441/v003t01a096-99-gt-424.pdf by guest on 28 September 2022

ABSTRACT

Local and global effects of cylindrical vortex generators on the mass transfer distributions over the four active walls of a square, rib-roughened rotating duct with a sharp 180° bend are investigated. Cylindrical vortex generators (rods) are placed above, and parallel to, every other rib on the leading and trailing walls of the duct so that their wake can interact with the shear layer and recirculation region formed behind the ribs, as well as the rotation-generated secondary flows. Local increases in near-wall turbulence intensity resulting from these interactions give rise to local enhancement of mass (heat) transfer. Measurements are presented for duct Reynolds numbers (Re) in the range 5000 - 30,000, and for rotation numbers in the range 0 to 0.3. The rib height-to-hydraulic diameter ratio (e/Dh) is fixed at 0.1, while the rib pitch-to-rib height ratio (P/e) is 10.5. The vortex generator rods have a diameter-to-rib height ratio (d/e) of 0.78, and the distance separating them from the ribs relative to the rib height (s/e) is 0.55. Mass transfer measurements of naphthalene sublimation have been carried out using an automated acquisition system and are correlated with heat transfer using the heat/mass transfer analogy. The results indicate that the vortex generators tend to enhance overall mass transfer in the duct, compared to the case where only ribs are present, both before and after the bend at high Reynolds and Rotation numbers. Local enhancements of up to 30% are observed on all four walls of the duct. At low Reynolds numbers (e.g. 5,000) the insertion of the rods often leads to degradation. At high Reynolds numbers (e.g. 30,000) the enhancement due to the rods occurs on the surfaces stabilized by rotation (trailing edge on the inlet pass and leading edge on the outlet pass) and the side walls.. The enhancement is more pronounced as the Rotation number is increased. The detailed measurements in a ribbed duct with vortex-generator rods clearly show localized regions of enhanced mass (heat) transfer at Reynolds and Rotation numbers within the envelope of practical interest for gas-turbine blade cooling applications.

INTRODUCTION

One of the primary goals in the development of advanced turbine systems is to explore more effective methods of heat removal from the turbine blades. This paper deals with the flow and heat transfer in the internally ribbed coolant channels of a rotating gas turbine blade and aims to examine heat transfer enhancement brought about by placing vortex generators above the ribs in the coolant passages. This expected enhancement is based on observations made in flow past ribs (Acharya et. al., 1991) in which it was shown that the separated shear layer behind the rib was characterized by vortical structures, and that these structures could be manipulated by introducing an external perturbation into the flow in order to promote mixing behind the rib. Greater mixing and shear layer growth behind the ribs is expected to lead to enhancement in surface heat transfer. In this paper the vortex street behind a cylindrical vortex generator mounted above the rib will be used as the external perturbation,

[1] Corresponding Author

Presented at the International Gas Turbine & Aeroengine Congress & Exhibition
Indianapolis, Indiana — June 7–June 10, 1999

and its effect on the heat transfer from the ribbed surface will be examined. The focus of this paper is to consider a realistic two-pass ribbed coolant channel geometry and to examine the effect of vortex generators under rotational conditions that are more representative of turbine blade cooling.

Numerous experimental investigations reporting the local and average heat transfer behavior in ribbed channels are available in the literature (e.g. Han and Zhang, 1991; Acharya et. al., 1993; Abuaf and Kercher, 1994; Acharya et. al., 1995a, 1995b; Taslim et al., 1998). In general, these studies consistently report significant heat transfer enhancement due to the ribs, with peak heat transfer values in the vicinity of reattachment and just upstream of the rib. Acharya et. al. (1994) have reported measurements of velocity and heat transfer past a surface mounted rib, and have shown the correlation between the surface heat transfer and near wall velocity fluctuations. Karniadakis, Mikic, and Patera (1988) performed a numerical study, and using the Reynold's Analogy of momentum and heat transfer, showed that heat transfer rate increases with flow instability.

In recent years, more effective heat removal techniques based on manipulating the flow structures in a shear layer or boundary layer have been explored. A half delta wing geometry has been shown to generate longitudinal vortices embedded in the boundary layer in such a way that heat transfer dominates over momentum transfer (Wroblewski and Eibeck, 1991). With this vortex generator geometry, it was shown that the maximum heat transfer occurred at low Reynolds numbers (Garimella and Eibeck, 1991). A small fence-like geometry placed opposite a ribbed wall was shown to reduce the occurrence of local hot spots in the fully-developed region by inducing a more uniform heat transfer distribution (Hung and Lin, 1992). A cylindrical vortex generator placed above and parallel to the ribs in a 5:1 stationary rectangular duct has been shown to significantly increase heat transfer at low Reynolds numbers (Myrum et. al., 1992, 1993, 1995). However, these studies were limited to two-dimensional rectangular channel geometries that are not representative of turbine blade cooling situations.

More recently, Hibbs et al. (1998) have presented the effects of the vortex generator in a stationary two-pass ribbed square coolant channel, that is more representative of blade cooling, and at low Re (= 5,000) they had reported enhancements in the surface heat transfer induced hy the presence of the vortex generators. However, the study of Hibbs et al. (1998) was limited to stationary-blade conditions. The present paper extends this earlier study to rotating situations of interest and relevance to the gas turbine industry.

The present study uses a mass transfer (napthalene sublimnation) technique in view of the convenience of using this technique under conditions of rotation. The heat-mass transfer analogy can then be used to deduce the corresponding heat transfer behavior. Heat transfer measurements, under conditions of rotation, are considerably more complex since they require the use of slip rings. Further, they only provide limited and rather sparse resolution, while the napthalene sublimation technique provides very detailed surface resolution. The napthalene sublimation technique, together with the heat-mass transfer analogy, has been widely used, and a recent review of mass/heat transfer measurements using this technique has been reported by Goldstein and Cho (1995). A few papers have recently been reported where the napthalene sublimation technique has been successfully used under conditions of rotation (Hibbs et al., 1996, Park and Lau, 1998).

EXPERIMENTAL FACILITY AND METHODS

A rotating test facility, is used to simulate the flow in serpentine blade-cooling ducts. This facility covers a wide range of rotation (Ro) and Reynolds (Re) numbers. The product of these parameters (RoRe) can be varied continuously between zero and 25,000. The highest value can be achieved at 550 RPM by pressurizing the flow to 150 psig.

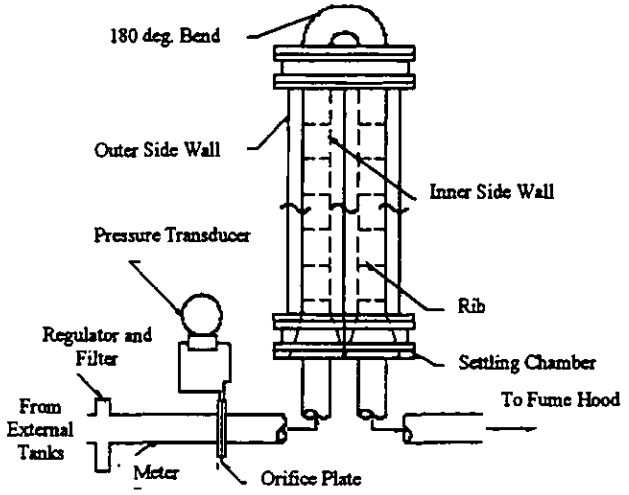

Figure 1: Schematic of the flow loop and test section

A schematic of the experimental flow loop used during this study is shown in Figure 1. This consists of an open air-flow loop connected to the test section and instrumented for flow-rate, pressure and temperature measurement of the air-stream. Compressed air is supplied at a steady pressure through a pressure regulator. Test-section pressure and flow control is achieved by means of ball valves placed downstream of the test section. Mass flow rate was measured in the meter run using a concentric bore orifice plate that is secured with orifice flanges. Free stream flow temperature was measured with a liquid-in-glass thermometer that has a readability of 0.25 °C.

The test section, which is an analog of a two-pass coolant channel, is schematically shown in Figure 2, consists of two 356-mm (14-in)-long ducts of square cross-section (25.4-mm × 25.4-mm, or 1-in × 1-in) connected by a 180^0 bend with a short radius of 16.5-mm (0.65-in) and a long radius of 42-mm (1.65-in.) The flow enters and leaves the test section through conically shaped transition sections. These sections provide for the transition from the circular crossection of the supply duct to the square test-section crossection and are quite short in length. It should be noted that other than these transition sections, no attempt to condition the flow is made. The flow is directed outwards (towards the bend) in one duct and inwards in the other after

Downloaded from http://asmedigitalcollection.asme.org/GT/proceedings-pdf/GT1999/78606/V003T01A096/2412441/v003t01a096-99-gt-424.pdf by guest on 28 September 2022

going around the bend. Details of the experimental facility can be found in Hibbs (1996).

As noted earler, heat transfer results in this study are deduced from the naphthalene-sublimation mass transfer technique. The test section consists of an aluminum frame that carries eight, 305-mm (12-in) removable plates that form its inner walls. Each plate provides a reinforced recessed frame to accommodate casting of a naphthalene layer for mass transfer measurements. Casting of the test-section wall-plates is done against highly polished stainless steel plates to provide a smooth and flat naphthalene reference surface.

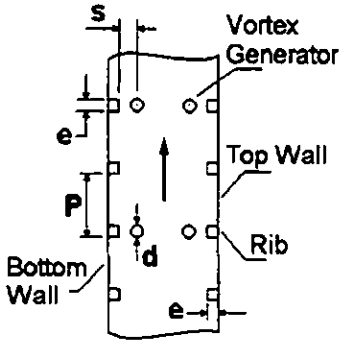

Figure 2: Schematic of ribbed duct with vortex generators.

Straight aluminum rib-turbulators 25.4-mm (1.0 in.) long and with a 2.54-mm x 2.54-mm (0.1 in. x 0.1 in.) square cross section (rib-side e=0.1) are placed at equal stream-wise increments (P) on the top and bottom plates and at 90° with respect to the flow direction for the ribbed channel studies (Figure 2). The ribs are not coated with naphthalene and therefore do not participate in the mass/heat transfer process.

The vortex generators are steel rods with diameter-to-rib height ratio, d/e = 0.78 and vortex generator to rib spacing, s/e=0.55. The side walls have holes of the same diameter as the vortex generator so the latter can slide-in through these holes. The vortex generators are placed directly above the rib, as shown in Figure 2, at the proper position, and at a pitch-to-rib height, P/e = 21. Leading and trailing walls are then fastened into place. It should be noted that we have also used a higher s/e=1.5 during our study, which did not yield results as promising as s/e=0.55.

The naphthalene-sublimation technique requires detailed measurements of the naphthalene surface profiles for each wall-plate of the test section. A computer driven profilometer is used in this study to obtain high resolution maps of the naphthalene surface on a pre-defined grid and measure the sublimation depth. The uncertainty of this measurement is of the order of 3.8-μm (0.00015-in.) and the positioning uncertainty is of the order of ± 7.6-μm (± 0.0003 in). Typical grid sizes were 840 points (30x28) for an inter-rib cell with the smallest pitch (P/e=10.5). The spatial resolution in the stream-wise direction was 3.8 pts/e (pts/e denoting points per rib height, e), and 4 pts/e in the span-wise direction. The naphthalene surface profiles for each wall were measured before and after each test. The difference between the normalized profiles gives the local sublimation depth, δ. The local sublimation mass flux $\dot{m}''$ at each location is calculated as, $\dot{m}'' = \rho_s \delta / \Delta t$, where ρ_s is the density of solid naphthalene, and Δt is the duration of the experiment. Vapor pressure at the wall p_w is calculated from Sogin's (1958) equation, $\log_{10}(p_w) = A - B/T_w$, where A and B are constants (with values of 11.884 and 6713, respectively) and T_w is the absolute wall temperature. Wall vapor density ρ_w is then calculated using the perfect gas law. Bulk vapor density of naphthalene $\rho_b(x)$ was calculated by integrating the mass flow rates of naphthalene from the inlet (x=0) to the stream-wise location (x) over the four active walls. The sublimation data from the duct centerline were used for this calculation. The bulk vapor density is assumed zero at the inlet and constant through the inactive bend. The local dimensionless mass transfer rate or Sherwood number Sh was calculated as:

$$Sh = h_m D_h / D_{n-a} = \left[\frac{\dot{m}''}{(\rho_w - \rho_b(x))}\right]\frac{D_h}{D_{n-a}} = \left[\frac{\dot{m}''}{(\rho_w - \rho_b(x))}\right]\frac{D_h}{\nu/Sc} \quad (1)$$

where D_h is the hydraulic diameter of the test section, h_m is the local mass transfer convection coefficient,. D_{n-a} is the binary diffusion coefficient for naphthalene sublimation in air, ν is the kinematic viscosity of air, and Sc=2.5 is the Schmidt number for naphthalene-air.

Heat transfer results can be deduced from the mass transfer results through the heat-mass transfer analogy (Sogin, 1958), $Nu = Sh(Pr/Sc)^{0.4}$, where Nu is the Nusselt number and Pr is the Prandtl number of air. The analogy is implicit in all consequent discussions of the experimental results where the Sherwood number is mentioned.

Uncertainty estimates for all computed values were computed using the second-power equation method (Kline and McClintock, 1953). The estimates for these experiments are comparable to previously reported values for both heat transfer and mass transfer studies, but are believed to be conservative. Volume flow rate and duct Reynolds number (Re) uncertainties were estimated to be less than 10 percent for Re>6000. Sublimation depths were maintained roughly at an average of about 254-μm (0.01 in.) by varying the duration of the experiment. This target depth was selected to minimize uncertainties in both depth measurement and changes in duct cross section area. These uncertainties were found to be 1 and 3 percent, respectively. The resulting experimental duration was between 90 minutes for Re=30,000 and 180 minutes for Re=5,000. Vapor density uncertainty based on measured quantities is negligible for both wall and bulk values. Overall uncertainty in Sherwood number calculation is about 8 percent and varies slightly with Reynolds number (<1 percent). The uncertainty in Reynolds number is 8% and 10% in Rotation number.

We have compared our naphthalene sublimation results with three past mass-transfer based studies (Kukreja et al., 1993; Chyu and Wu, 1989 and Han et al., 1988) as well as two previous heat-transfer studies (Han and Park, 1988 and Liou and Hwang,

Downloaded from http://asmedigitalcollection.asme.org/GT/proceedings-pdf/GT1999/78606/V003T01A096/2412441/v003t01a096-99-gt-424.pdf by guest on 28 September 2022

1992b). These comparisons have been documented in Chen et al. (1996). The agreement between our measurements and all of these other studies was in general very good (within experimental uncertainty). We are presenting here only a representative case in Figure 3, where our data are compared with measurements of average Nusselt numbers obtained with a laser holographic interferometric technique by Liou and Hwang (1992b) in a ribbed duct at various Reynolds numbers.

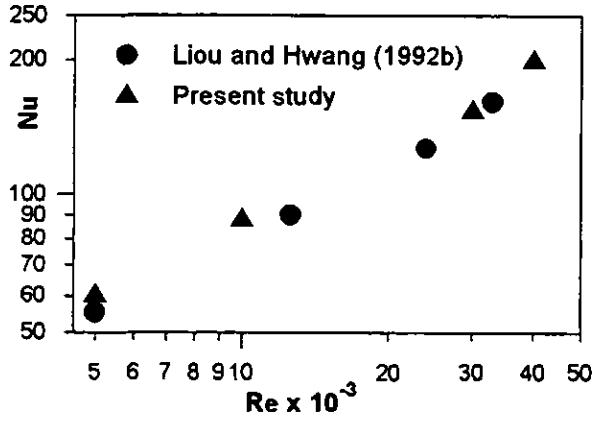

Figure 3: Comparison of average Nusselt numbers as a function of Reynolds number from the present study in a ribbed channel, with e/Dh=0.1, and P/e=10.5, with those of Liou and Hwang (1992b).

RESULTS AND DISCUSSION

High-resolution experimental mass-transfer results for the ribbed, two-pass, square channels with cylindrical vortex generators under stationary and rotating conditions, are presented in the following sections. These results are compared to those for the corresponding channels with ribs only. The experiments were performed at Re=5,000, 10,000, 20,000, 30,000 and Ro=0.0, 0.1, 0.2, 0.3 for both rib-only and rib-rod vortex generator geometries. The data are primarily presented in terms of cell-averaged Sherwood number ratios (Sh/Sh_o) for each side of the inlet and outlet channels, as functions of Re and Ro. The reference Sherwood number Sh_o is that for smooth stationary channels, as obtained from the McAdams (1954) correlation. The cell-averages were computed for the "periodically fully developed" cells. The detailed mass-transfer distributions over these "fully-developed" cells and the first cell after the 180 deg bend, are presented and discussed for selected cases of low (5,000) and high (30,000) Re, and zero and high (0.3) Ro.

Before discussing the effects of Re and Ro numbers on the mass-transfer for the rib-only and rib-rod geometries, some of the salient features of the Sherwood number distribution in a typical module will be described. . To this end, centerline distributions of the Sherwood number ratio for the leading and trailing walls of the inlet (flow away from the axis of rotation) and outlet (flow towards the axis of rotation) ducts are presented in Figure 4 at high Reynolds (30,000) and Rotation (0.3) numbers. A two-rib-pitch module is shown only between successive vortex generators (rod), because the pattern repeats itself in the "periodically developed" region. It is observed that on the walls destabilized by the effect of rotation, degradation (relative to the rib-only case) occurs immediately after the vortex-generator bearing rib. This is followed by an increase in mass transfer leading to enhancement prior to the downstream rib (with no vortex generator). The peak mass transfer in the inter-rib module therefore occurs close to the downstream rib, and implies that the rib-rod element may act as a single taller rib with reattachment further downstream than the rib-only case. It is most likely that the flow between rib and rod is inhibited leading to this behavior. The module after the no-generator rib shows predominantly degradation relative to the rib-only case. On the stabilized walls, the presence of the vortex generators leads to mass transfer enhancement downstream of the rib-rod element in the majority of the intra-rib space. This enhancement is also sustained downstream of the plain rib as well. It can be concluded from this consistent and periodic pattern at high Re and Ro numbers that the presence of the vortex generators favors the stabilized walls while being detrimental to the destabilized walls of the rotating coolant channel. As a result, the differences in heat transfer between the leading and trailing walls are smaller in the presence of vortex generators.

Averaged Mass Transfer Data

The dependence of the cell-averaged Sherwood number ratio (Sh/Sh_o) on the Rotation number, Ro, is shown in the first row of graphs of Figure 5 for the highest Reynolds number, Re=30,000. The second row of graphs of Figure 5 show the dependence of the cell-averaged Sherwood number ratio (Sh/Sh_o) on the Reynolds number for Ro=0.3. The first two columns of graphs in this figure refer to the inlet duct (flow direction is away from the axis of rotation), and the last two rows refer to the outlet duct (flow direction towards the axis of rotation). Both the baseline rib-only (denoted as RO in the figure) and rib-vortex generator (RO+VG in the figure) cases are presented.

Rotation Number Effects at High Reynolds Number

At Ro=0.0 (stationary case) a slight difference in mass transfer ratios is observed between the leading and trailing walls in the inlet duct for the baseline case. This can be attributed to an asymmetry in the inlet flow profile. A small asymmetry can also be seen on the side walls of the outlet duct, possibly due to the remains of the secondary flows induced by the bend, which tend to drive the flow outwards. The rest of the walls show the expected symmetry under non-rotating conditions.

For the baseline (rib-only) case, the Sherwood number ratio along both leading and trailing walls of the inlet duct increase monotonically up to Ro=0.2. The trailing wall displays higher mass transfer ratios than the leading wall, as expected, due to the Coriolis induced secondary flows that drive cooler mainstream flow toward the trailing side of the inlet duct. The Coriolis forces also tend to destabilize the shear layer or boundary layer along the trailing edge and stabilize it along the leading edge. Between Ro=0.2 and Ro=0.3 the ratio along the trailing wall ratio continues to increase but at a lower rate while the ratio along the leading wall decreases. The exact opposite phenomenon is observed in the outlet duct, where the leading wall ratio increases

Downloaded from http://asmedigitalcollection.asme.org/GT/proceedings-pdf/GT1999/78606/V003T01A096/2412441/v003t01a096-99-gt-424.pdf by guest on 28 September 2022

with Ro, and the trailing wall ratio reaches a peak at Ro=0.2, and then decreases sharply. The leading wall displays higher mass transfer ratios than the trailing wall, again due to the Coriolis induced secondary flows and the destabilizing/stabilizing effects along the leading/trailing surfaces of the outlet duct.

Based on the observations outlined above it appears that for the leading wall in the inlet duct and the trailing wall in the outlet duct a somewhat "anomalous" or non-monotonic behavior exists across Ro=0.2. Strong evidence of this non-monotonic behavior also exists in the distributions of the Sherwood number ratio along the side walls. Again, for the baseline (rib-only) case, the mass transfer ratio along both side walls in the inlet duct grows monotonically up to Ro=0.2. Beyond that point, the outer wall ratio declines while the inner wall ratio continues to increase. Furthermore, the relative magnitudes of outer and inner wall mass transfer ratios change sign from Ro=0.2 (outer higher than inner) to Ro=0.3 (inner higher than outer). The exact same qualitative trend is observed for the side walls of the outlet duct. In order to confirm the non-monotonic behavior observed, the experiments were repeated several times, and the observed trends were always repeatable. Therefore there is a high degree of confidence that the non-monotonic behavior observed across Ro=0.2 are indeed real. In examining the published data, as in the present study, the behavior along the leading edge of the inlet duct and that along the trailing edge of the outlet duct has been reported to be more complex than that along the opposite surfaces. Non-monotonic behavior with increasing Ro has been reported with an initial decrease followed by an increase due to centrifugal buoyancy (Wagner et al., 1992), as well as an initial increase followed by a decrease due to changes in the flow pattern (Dutta et al., 1996). In the absence of flow data, and the measured details of the complex strongly three-dimensional flow field, only a speculative explanation can be given at this time. The change in behavior observed across Ro=0.2 is related to a change in the nature of the secondary flows in the duct. At low Rotation numbers the Coriolis-induced secondary flows may still be competing with the secondary flows induced by the turbulent-stresses in the non-circular channel. Coriolis forces may augment stress anisotropies which, in turn, may enhance the stress driven secondary flows and thus promote the surface mass transfer. At high Rotation numbers this competition may be clearly in favor of the Coriolis-induced secondary flows that leads to a reduction of mass transfer along the stabilized surface (leading surface along the inlet and trailing surface along the outlet). This competitive mechanism may also be responsible for the overall enhancement of mass (heat) transfer observed with increasing Rotation number, particularly in the range 0-0.2. To examine the dependence of mass transfer on Ro, we have computed four-wall averages combining data from both inlet and outlet channels in the fully developed region. We found that these average values of the Sh/Sho ratio have a relatively weak dependence on Re within the range of our experiments for Re>5,000. We also found that the dependence of Sh/Sh_o ratio on Ro number is of the form $a+bRo^{0.51}$. This was so both for the rib-only case and the one with vortex generators; each case yields different constants a and b of similar order of magnitude. The data we have is rather limited to yield reliable constants. However, it is worth noting that the dependence of the Sh/Sh_o on Ro is approximately a square-root one.

Although the qualitative trends of the Rotation number dependence are similar between inlet and outlet ducts, quantitative differences are observed. These differences can be attributed to a long lasting effect of the bend and the reversal of the flow direction. Essentially the spatial distributions of the flow-field "initial" conditions for the inlet and outlet ducts are quite different.

The anomalous non-monotonic behavior noted above seems to be reinforced by the results of the case where vortex generators are used. The presence of the vortex generators is certainly capable of influencing the details of the secondary flows in the channel. Thus, qualitative changes should be expected, and are observed. For instance, in the inlet duct at low Ro (<0.1) the presence of the vortex generators influences the mass transfer ratio very little. However, at high Ro (≥ 0.2) the effect is substantial resulting in degradation of mass transfer and the replacement of the stabilized (leading) wall peak at Ro=0.2 by a minimum. At Ro=0.3 the destabilized (trailing) surface displays degradation while the stabilized (leading) one shows enhancement, and as a consequence the mass transfer rates from the leading and trailing surfaces are closer to each other with vortex generators. This may be due to the disruption of the rotation induced secondary flows by the presence of the vortex generators. Along the outlet duct also, the differences in mass transfer between the leading and trailing surfaces are lower at Ro=0.3. The side walls mostly display mass transfer enhancement when vortex generators are included, with the exception of the Ro=0.2 case where enhancement is observed only along the inner wall. Again the presence of an anomalous behavior at the neighborhood of Ro=0.2 points towards the existence of a threshold condition.

Reynolds Number Effects at High Rotation Number

It is seen from the bottom row of graphs on Figure 5 that the effect of the Reynolds number on the mass-transfer ratio is significant at low Reynolds numbers for the baseline (rib-only) case. All sides of both ducts display a sharp decrease in mass-transfer ratio between Re of 5,000 to 10,000. Note that it is the mass transfer ratio (normalized with respect to the smooth channel correlation) that decreases with Re and not the mass transfer itself, indicating that the ribbed duct has a weaker dependence on the Re than the normalizing smooth channel correlation. At higher Re, the Sherwood number ratios tend to increase again.

The Reynolds number dependence of the rib-rod case appears to be considerably weaker than the rib-only case. Severe mass transfer degradation is experienced at low Reynolds numbers for all sides of both inlet and outlet ducts. Enhancement is observed as the Reynolds number increases particularly for the side walls. At the highest Reynolds number some enhancement is seen on the stabilized walls of the inlet and outlet ducts.

Downloaded from http://asmedigitalcollection.asme.org/GT/proceedings-pdf/GT1999/78606/V003T01A096/2412441/v003t01a096-99-gt-424.pdf by guest on 28 September 2022

Comparison Between Rib-Rod and Rib-Only Results

Table 1a gives a comparison between the rib-rod case and the rib-only at Re=30,000 and with Ro varying from 0.0 to 0.3 at 0.1 intervals. The comparison was made by averaging the two consecutive periodically fully-developed cells. As it can be observed, mass transfer enhancement is achieved by the use of vortex generators on the stabilized walls for the highest rotation number only, while degradation occurs on the destabilized walls. The side walls show enhancement at Ro of 0.1 and 0.3.

In Table 1b the comparison is made for fixed Ro=0.3 and varying Re from 5,000 to 30,000. Degradation is observed on all walls at low Reynolds numbers. This degradation decreases with increasing Reynolds number. At the highest Re=30,000 enhancement can be reported in all walls except those destabilized by rotation.

The results seem to imply that the performance of vortex generators in improving mass transfer becomes better as both the Reynolds and Rotation numbers are increased.

Detailed Mass-Transfer Distributions

Figures 6-11 show detailed Sherwood number ratio results in the form of constant Sh/Sh_o contours. These are presented in the figures, for two "fully-developed" cells in the inlet duct, the cell following the 180 deg bend, and a pair of two "fully-developed" cells in the outlet duct. In analysing these figures it should be noted that the vortex generators are placed on alternate ribs, and in the pair of fully developed cells shown, there is no vortex-generator upstream of the first cell while there is a vortex generator upstream of the second cell. The contours in figures 6, 8, and 10 are for the baseline case without vortex generators (henceforth referred to as rib-only cases). High-Reynolds number stationary results (Re=30,000, Ro=0.0) are shown in Figure 6, high-Reynolds number with rotation results (Re=30,000, Ro=0.3) are presented in Figure 8, and low-Reynolds number with rotation results are depicted in Figure 10. The rib-only results are included here as a baseline case to compare with the corresponding cases where vortex generators were present (henceforth referred to as rib-rod cases). The detailed Sherwood number ratio results in the form of constant Sh/Sh_o contours for these cases are presented in Figures 7, 9, and 10.

Comparison between Figures 6 and 7, for the stationary case, indicate that the major effect of the presence of vortex generators is one similar to that produced by a higher rib. It is evident, by comparing the second fully developed cell of the leading and trailing surfaces in both the inlet and outlet duct, that the reattachment location behind the ribs with vortex generators has been pushed downstream and probably straddles the next rib. The same evidence exists in the after-bend module in the outlet duct. Indeed a region of maximum mass transfer indicative of reattachment is visible in the rib-only case while it is absent in the rib-rod case. This is the main reason why the rib-rod case fails to produce mass-transfer enhancement in this module. The absence of reattachment behind the vortex-generator bearing rib is also visible on the side walls of the corresponding module. The "wake" regions behind the vortex-generator bearing ribs are considerably larger in the rib-rod case extending closer to the downstream rib. This "wake" region manifests itself as a single structure, indicating that flow through the gap between the rib and the vortex generator is very weak, if non-existent. The same can be deduced by the signature of a single recirculation zone on the side walls ahead of the vortex-generator bearing rib. Considerable enhancement is observed behind the vortex-generator bearing ribs both in the larger "wake" region and the central region of the wall. The latter region is enhanced probably due to the acceleration of the mean flow caused by the increased blockage as well as the turbulence enhancement caused by the presence of the vortex generator.

In the module upstream of the vortex-generator, the maximum in the mass transfer ratio associated with reattachment can be clearly observed for both the leading and trailing walls of the inlet and outlet ducts. Thus the general nature of the flow pattern in this upstream module is comparable with that in a rib-only module case. However, there are observable differences in the patterns and in the magnitudes between the rib-rod and rib-only cases and are the consequences of the vortex generator located in the previous. For the side walls ahead of the vortex-generator bearing rib, the rib-rod case shows significant enhancement in this region. This is most likely due to increased turbulent intensity introduced by the vortex generator upstream that is transported downstream. In the module after the bend, the bend effects that induce secondary flow from the inner to the outer surface, can be observed. This effect seems to be more prominent for the rib-rod case, where the Sherwood number ratio on the outer wall are higher than that along the inner wall.

Figures 8 and 9 presents the detailed mass-transfer ratio data for the rotating cases, and show the basic features of the Coriolis effect. For both rib-only and rib-rod cases, the stabilized wall is subject to lower mass transfer ratios than the destabilized wall. The same signature exists on the side walls. The half of the side wall towards the stabilized side has lower mass transfer ratios than the other half adjacent to the destabilized wall. In the shear-layer regions behind the ribs and in the "wakes" of the vortex generators, the Coriolis-effect leads to substantially diminished Sherwood number ratios on the stabilized wall side and substantially enhanced ratios on the destabilized side.

The same salient features as for the stationary cases are observed in terms of the rib and vortex generator effects. The comparison between the rib-only and rib-rod cases also shows that in the module after the vortex-generator bearing rib, the presence of the vortex generators seem to reduce the asymmetry between leading and trailing walls caused by the Coriolis effect. This is also indicated by the averaged data in Figure 5 and can be attributed to the possible disruption, caused by the vortex generators, of the secondary flows induced by rotation. In the module after the bend, the general trends, caused by the presence of the bend, that have been discussed in the previous section are present in the rib-only case. In the rib-rod case (Figure 9) a vortex-generator exists over the first rib after the bend. Its presence dominates in defining the qualitative features of the mass transfer distribution. However, the bend effect is still visible by virtue of the asymmetry between the outer and inner

Downloaded from http://asmedigitalcollection.asme.org/GT/proceedings-pdf/GT1999/78606/V003T01A096/2412441/v003t01a096-99-gt-424.pdf by guest on 28 September 2022

walls. The outer wall shows higher overall mass transfer than the inner one. Also the strong asymmetry between leading and trailing walls perpetrated by Coriolis effects and observed in the after-bend module for the rib-only case is absent in the rib-rod case. This can be attributed to the presence of the vortex generator which may disrupt the local secondary flow patterns emerging from the bend. It is also noteworthy that the minimum in mass-transfer ratio observed in the central region of the inner wall after the bend is considerably smaller when vortex generators are present (approximately 0.4 in the rib-rod case rather than 1 for the rib-only case).

The qualitative features discussed above for the high Reynolds number case with rotation are essentially the same at Low Reynolds number under the same rotation number. This is evident when comparing Figures 10 and 11 (Re=5,000, Ro=0.3) with 8 and 9 respectively.

CONCLUDING REMARKS

High-resolution experimental mass-transfer results for ribbed, two-pass, square channels with cylindrical vortex generators under stationary and rotating conditions have been presented and discussed. These results have been compared to those for the corresponding channels with ribs only. Based upon the discussion and comparisons of these results the following conclusions can be drawn:

1. When placed directly above the ribs, vortex generators seem to produce results that would be expected from a taller rib. Effects of flow through the gap between the vortex generator and the rib do not seem to be present.
2. The Coriolis effect is dominant in all rotating cases. The presence of vortex generators tends to reduce the asymmetry caused by rotation between stabilized and destabilized walls.
3. Vortex generators appear to be effective at high Reynolds and Rotation numbers.
4. The results with vortex generators indicate that the mass transfer in the ducts is less sensitive to the Reynolds number compared to the rib-only duct.
5. The vortex generators cause severe mass transfer degradation at low Reynolds and Rotation numbers.
6. Vortex generators are more effective in enhancing mass transfer on the side walls of the ducts.
7. Vortex generator use may be more effective on the stabilized walls of the rotating ducts.

ACKNOWLEDGMENTS

This research was performed under a subcontract from the South Carolina Energy Research and Development Center to Louisiana State University (93-01-SR015). The contract monitors were Dr. Daniel Fant and Dr. Larry Golan. Their help is gratefully acknowledged.

REFERENCES

Abuaf, N., and Kercher, D. M., 1994, "Heat Transfer and Turbulence in a Turbulated Blade Cooling Circuit," *J. of Turbomachinery*, Vol. 116, pp. 169-177.

Acharya, S., Myrum, T., and Inamdar, S., 1991, "The Effect of Subharmonic Flow Pulsation in a Ribbed Pipe: Flow Visualization and Pressure Measurements", *AIAA Journal*, Vol. 29, 9, pp.1390-140

Acharya, S., Dutta, S., Myrum, T., and Baker, R. S., 1993, "Periodically Developed Flow and Heat Transfer in a Ribbed Duct", *Int. J. Heat and Mass Transfer*, Vol. 36, 8, pp.2069-2082

Acharya, S., Dutta, S., Myrum, T., and Baker, R. S., 1994, "Turbulent Flow Past a Surface Mounted Rib", *J. Fluids Engng.*, Vol. 116, 2, pp. 238-246

Acharya, S., Myrum, T., Sinha, S., and Qiu, X., 1995a, "Developing and Periodically Developed Flow, Temperature and Heat Transfer in a Ribbed Duct", *Int. J. Heat Mass Transfer*, 1997, Vol. 40, 2, pp. 461-480

Acharya, S., Myrum, T. A., and Dutta, S., 1995b, "Heat Transfer in Turbulent Flow Past a Surface Mounted Two-dimensional Rib", *ASME IMEC&E.*, San Francisco, November 1995.

Chen, Y., Nikitopoulos, D. E., Hibbs, R., Acharya, S., and Myrum, T. A., 1996, "Detailed Mass Transfer Distribution in a Ribbed Coolant Passage", ASME Paper 96-WA/HT-11.

Chyu, M. K., and Wu, L. X., 1989, "Combined effects of rib angle-of-attack and pitch-to-height ratio on mass transfer from a surface with transverse ribs," *Experimental Heat Transfer*, Vol. 2, pp. 291-308.

Dutta, S., J-C, and Lee, C. P., "Local heat transfer in a rotating two-pass ribbed triangular duct with two model orientations", *Int. J. of Heat and Mass Transfer*, Vol. 39, No.4, pp. 707-715.

Durst, F., Founti, M., and Obi, S., 1988, "Experimental and Computational Investigation of the Two-dimensional Channel Flow over Two Fences in Tandem," *J. Fluids Engineering*, Vol. 110, pp. 48-54.

Garimela, S. V., and Eibeck, P. A., 1991, "Enhancement of Single Phase Convective Heat Transfer from Protruding Elements Using Vortex Generators," *Int. J. Heat Mass Transfer*, Vol. 34, 9, pp. 2431-2433.

Goldstein, R. J., and Cho, H. H., 1995, "A Review of mass Transfer measurements Using Napthalene Sublimation", *Experimental Thermal and Fluid Science*, Vol. 10, pp. 416-434

Han, J. C., and Park, J. S., 1988, "Developing Heat Transfer in Rectangular Channels with Rib Turbulators" *Int. J. of Heat and Mass Transfer*, vol. 31, 1, pp. 183-195.

Han, J. C., and Zhang, P., 1991, "Effect of Rib-Angle Orientation on Local Mass Transfer Distribution in a Three-pass Rib-roughened Channel," *J.of Turbomachinery*, Vol.113, pp.123-130.

Hibbs G. R., 1996, "Vortex Generator Induced Heat Transfer Enhancement In Gas Turbine Coolant Channel," MS Thesis, LSU.

Hibbs, R., Acharya, S., Chen, Y., and Nikitopoulos, D., "Heat/Mass Transfer in a Two-Pass Rotating Smooth and Ribbed Channel", *National Heat Transfer Conf.*, Houston, August 1996

Hung, Y. H., and Lin, H. H., 1992, "An Effective Installation of Turbulence Promoters for Heat Transfer Augmentation in a Vertical Rib-heated Channel," *Int. J. Heat Mass Transfer*, Vol. 35, 1, pp. 29-42.

Downloaded from http://asmedigitalcollection.asme.org/GT/proceedings-pdf/GT1999/78606/V003T01A096/2412441/v003t01a096-99-gt-424.pdf by guest on 28 September 2022

Karniadakis, George E., Mikic, Bora B., and Patera, Anthony T., 1988, "Minimum-dissipation Transport Enhancement by Flow Destabilization: Reynolds' Analogy Revisited," *J. Fluid Mech.*, Vol. 192, pp. 365-391.

Kline, S. J., and McClintock, F. A., 1953, "Describing Uncertainties in Single-sample Experiments," *Mech. Engineering*, Vol. 75, 1, pp. 3-8.

Kukreja, R. T., Lau, S. C., McMillin, 1992, "Local heat/mass transfer distribution in a square channel with full and V-shaped ribs," *Int. J. Heat Mass Transfer*, Vol. 36, 8, pp. 2013-2020.

Liou, T. M., Chang, Y., and Hwang, D. W., 1990, "Experimental and Computational Study of Turbulent Flows in a Channel with Two Pairs of Turbulence Promoters in Tandem," *J. Fluids Engineering*, Vol. 112, pp. 302-310.

McAdams, W., 1954, Heat Transmission, 3 rd. Ed., New York, McGraw-Hill Publishing Co.

Myrum, T. A., Acharya, S., Inamdar, S., and Mehrotra, A., 1992, "Vortex Generator Induced Heat Transfer Augmentation Past a Rib in a Heated Duct Air Flow," *J. Heat Transfer*, Vol. 114., pp. 280-284.

Myrum, T. A., Qiu, X., and Acharya, S., 1993, "Heat Transfer Enhancement in a Ribbed Duct Using Vortex Generators," *Int. J. Heat Mass Transfer*, Vol. 36, 14, pp. 3497-3508.

Myrum, T., Acharya, S., Sinha, S., and Qiu, X., 1996, "Flow and Heat Transfer in a Ribbed Duct with Vortex Generators", *Journal of Heat Transfer*, Vol. 118, 2, pp. 294-300.

Park, C. W., and Lau, S. C., 1998, "Effect of Channel Orientation of Local Heat (Mass) Transfer Distributions in a Rotating Two-Pass Square Channel with Smooth Walls", *J. of Heat Transfer*, Vol. 120, 3, pp. 624-632

Sogin, H. H., and Providence, R. I., 1958, "Sublimation from Disks to Air Streams Flowing Normal to Their Surfaces," *Transactions of the ASME*, Vol. 80, pp. 61-69.

Taslim, M. E., Li, T., and Spring, S. D., 1998, "Measurements of Heat Transfer Coefficients and Friction Factors in Passages Rib-Roughened on All Walls", *J. of Turbomachinery*, Vol. 120, pp. 564-570.

Wagner, J.H., Johnson, B.V., Graziani, R.A., and Yeh, F.C., 1992, "Heat Transfer in rotaiting serpentine passages with trips normal to the flow", *J. of Turbomachinery*, Vol. 114, pp. 847-857.

Wroblewski, Donald E., and Eibeck, Pamela A., 1991, "Measurements of Turbulent Heat Transport in a Boundary Layer with an Embedded Streamwise Vortex," *Int. J. Heat Mass Transfer*, Vol. 34, 7, pp. 1617-1631.

Zukauskas, A., 1994, "Enhancement of Forced Convection Heat Transfer in Viscous Fluid Flows," *Int. J. Heat Mass Transfer*, Vol. 37, Suppl. 1., pp. 207-212.

Wall #	Ro=0.0		Ro=0.1		Ro=0.2		Ro=0.3	
	Inlet	Outlet	Inlet	Outlet	Inlet	Outlet	Inlet	Outlet
Leading	0.86	0.94	0.94	1	0.64	1	1.12	0.84
Trailing	0.79	0.87	1.03	0.88	0.77	0.84	0.85	1.12
Outer	1.02	0.84	1.15	1.46	0.83	0.77	1.11	1.18
Inner	0.87	0.63	1.16	1.62	1.17	0.93	1.13	1.2

Table 1a. Fully-Developed Cell Average Comparison Between Rib-Rod Vortex Generator and Rib-Only Baseline Measurement at Re=30,000, s/e=0.55, P/e=10.5, e/Dh=0.1, d/e=0.78.

Wall #	Re=5,000		Re=10,000		Re=20,000		Re=30,000	
	Inlet	Outlet	Inlet	Outlet	Inlet	Outlet	Inlet	Outlet
Leading	0.74	0.63	0.97	0.98	0.66	1.07	1.12	0.84
Trailing	0.75	0.32	0.85	0.92	0.97	0.78	0.85	1.12
Outer	0.75	0.55	1.02	0.91	1.45	1.51	1.11	1.18
Inner	0.62	0.57	0.8	0.83	0.92	0.65	1.13	1.2

Table 1b. Fully-Developed Cell Average Comparison Between Rib-Rod Vortex Generator and Rib-Only Baseline Measurement at Ro=0.3, s/e=0.55, P/e=10.5, e/Dh=0.1, d/e=0.78.

Downloaded from http://asmedigitalcollection.asme.org/GT/proceedings-pdf/GT1999/78606/V003T01A096/2412441/v003t01a096-99-gt-424.pdf by guest on 28 September 2022

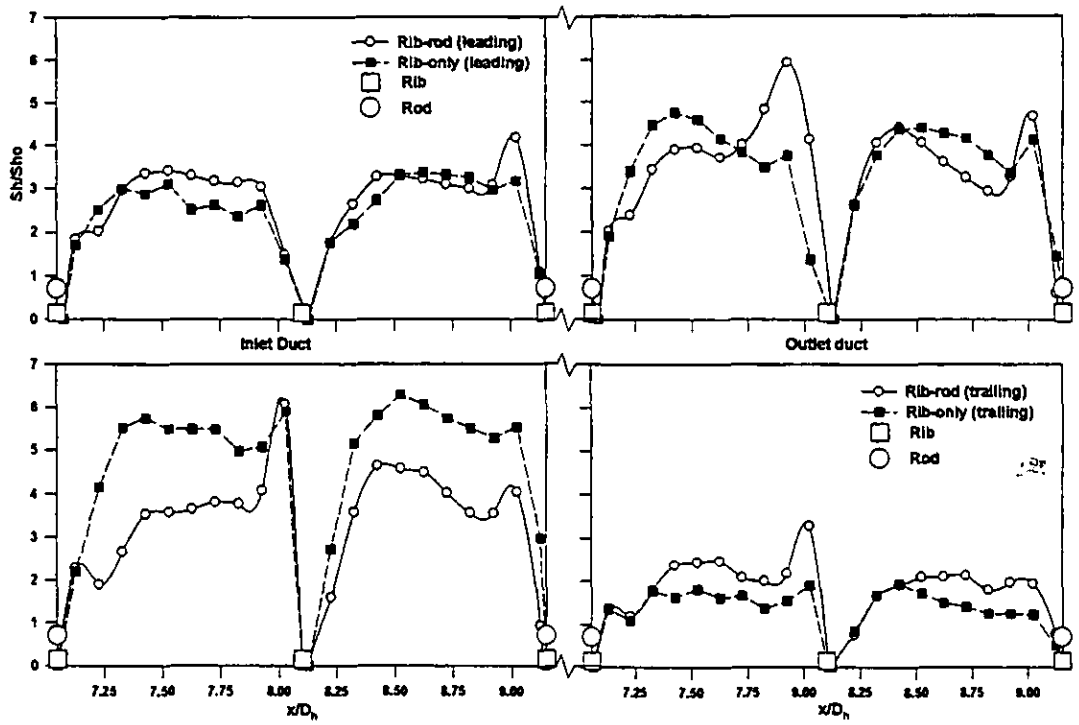

Figure 4: Centerline distributions of Sh/Sh_o for ducts with ribs only and rib-rod (s/e=0.55, d/e=0.78) geometries Re=30,000, Ro=0.3, e/D_h=0.1, P/e=10.5.

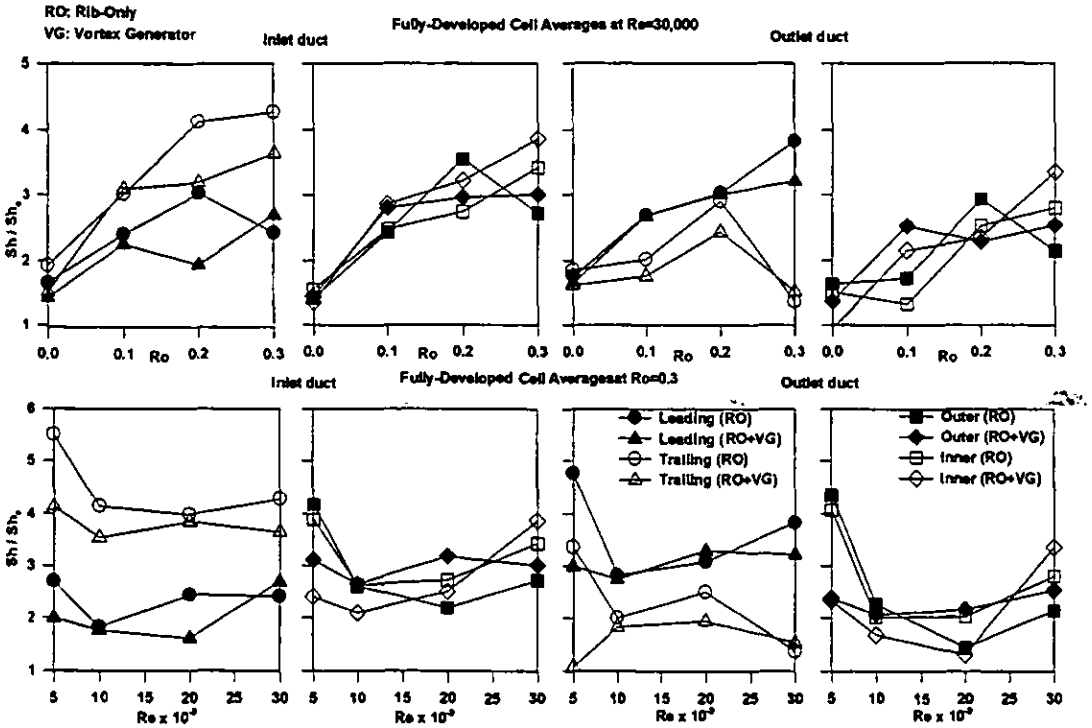

Figure 5: Fully-Developed Cell Averages of Sh/Sh_o at different rotation (Ro) and Reynolds (Re) numbers. P/e=10.5, e/D_h=0.1, d/e=0.78, s/e=0.55.

Downloaded from http://asmedigitalcollection.asme.org/GT/proceedings-pdf/GT1999/78606/V003T01A096/2412441/v003t01a096-99-gt-424.pdf by guest on 28 September 2022

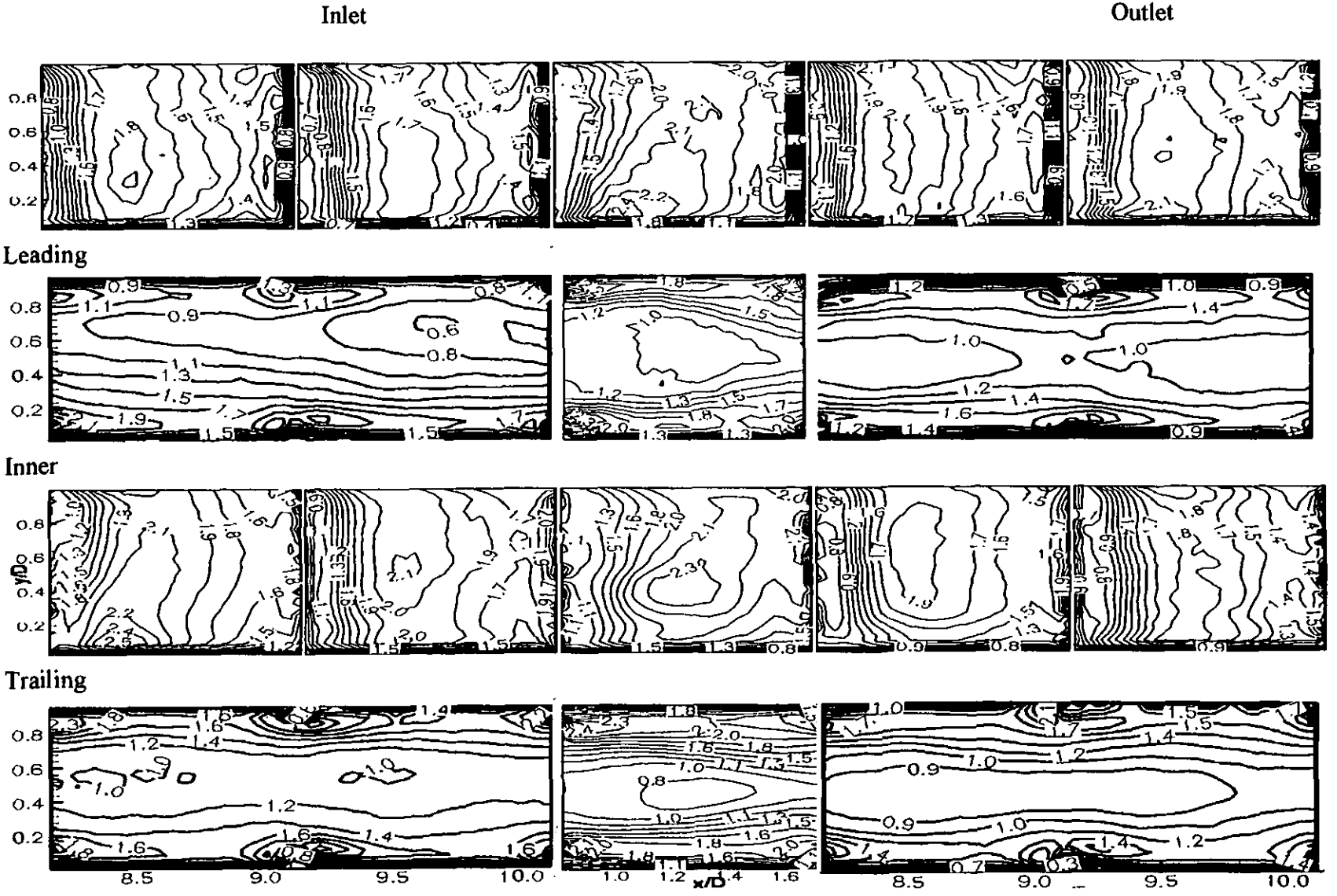

Figure 6: Detailed Sherwood Number Ratio Distributions Sh / Sho in Selected Developing and Fully-Developed Regions for the Ribbed Duct at Re=30,000, Ro=0.0, P / e=10.5, e / D_h=0.1.

Downloaded from http://asmedigitalcollection.asme.org/GT/proceedings-pdf/GT1999/78606/V003T01A096/2412441/v003t01a096-99-gt-424.pdf by guest on 28 September 2022

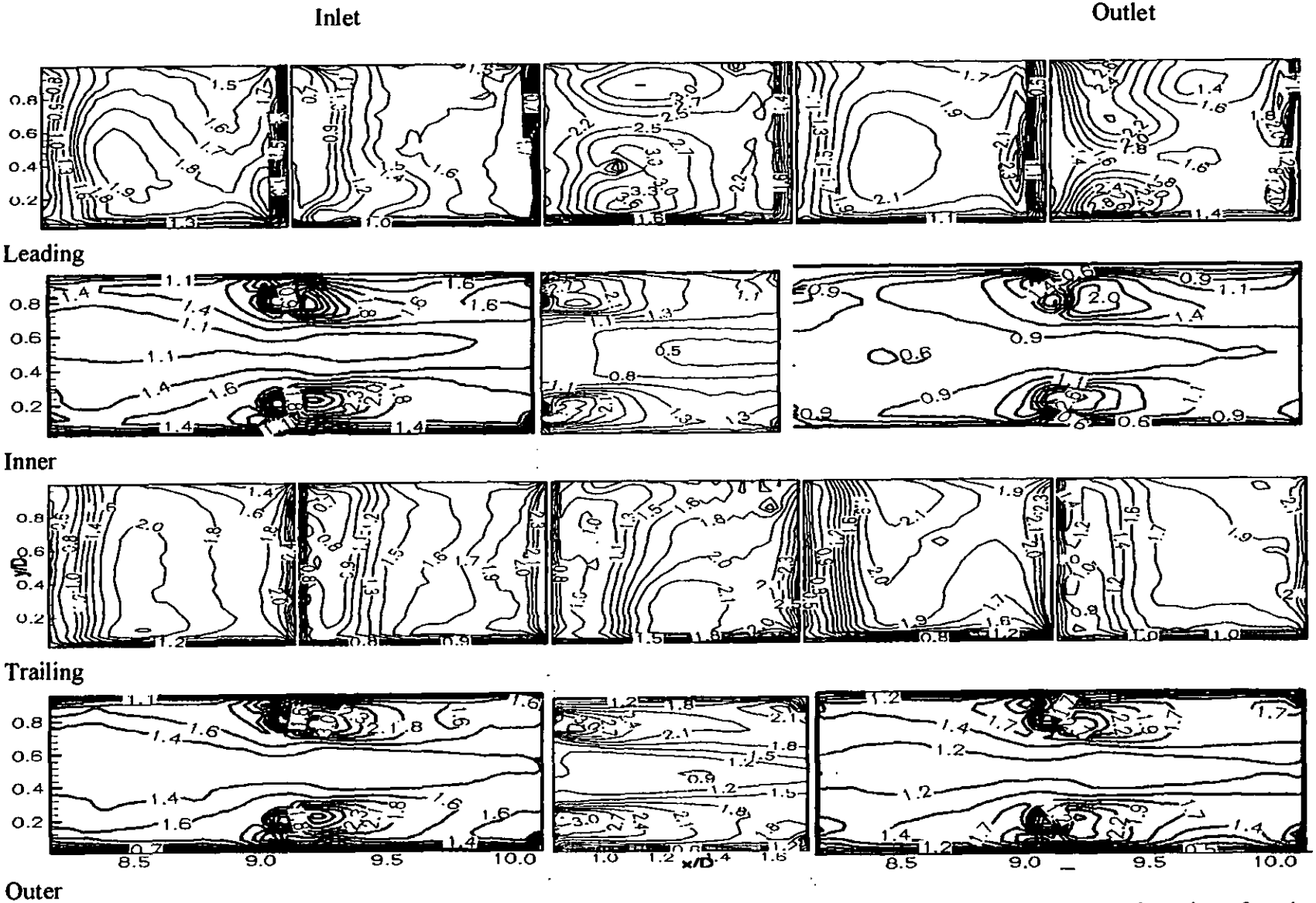

Figure 7: Detailed Sherwood Number Ratio Distributions Sh / Sho in Selected Developing and Fully-Developed Regions for the Ribbed Duct with Horizontal Rod Vortex Generators at Re=30,000, Ro=0.0, s / e=0.55, P / e=10.5, e / D_h=0.1, d / e=0.78.

Downloaded from http://asmedigitalcollection.asme.org/GT/proceedings-pdf/GT1999/78606/V003T01A096/2412441/v003t01a096-99-gt-424.pdf by guest on 28 September 2022

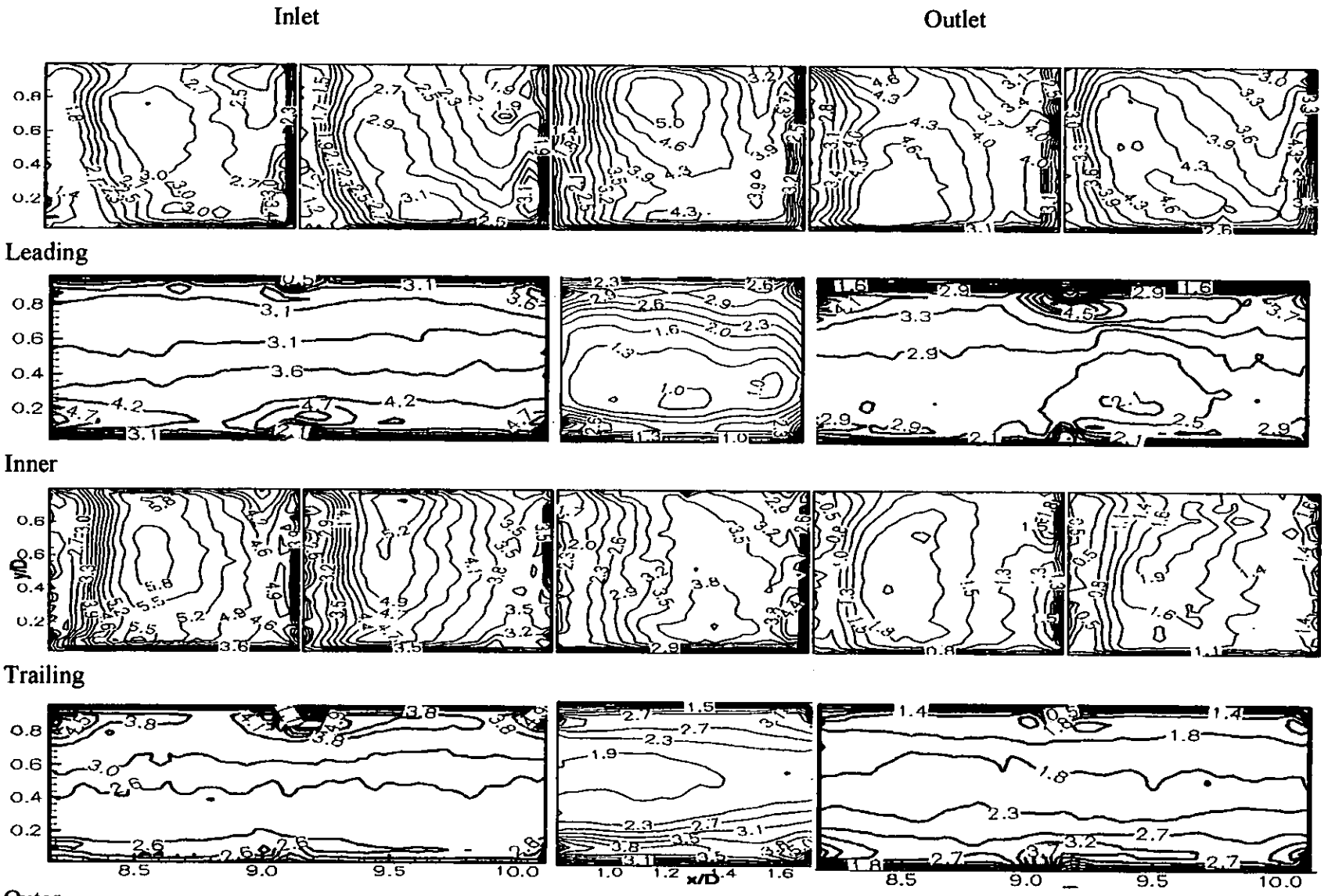

Figure 8: Detailed Sherwood Number Ratio Distributions Sh / Sh_o in Selected Developing and Fully-Developed Regions for the Ribbed Duct at Re=30,000, Ro=0.3, P / e=10.5, e / D_h=0.1.

Downloaded from http://asmedigitalcollection.asme.org/GT/proceedings-pdf/GT1999/78606/V003T01A096/2412441/v003t01a096-99-gt-424.pdf by guest on 28 September 2022

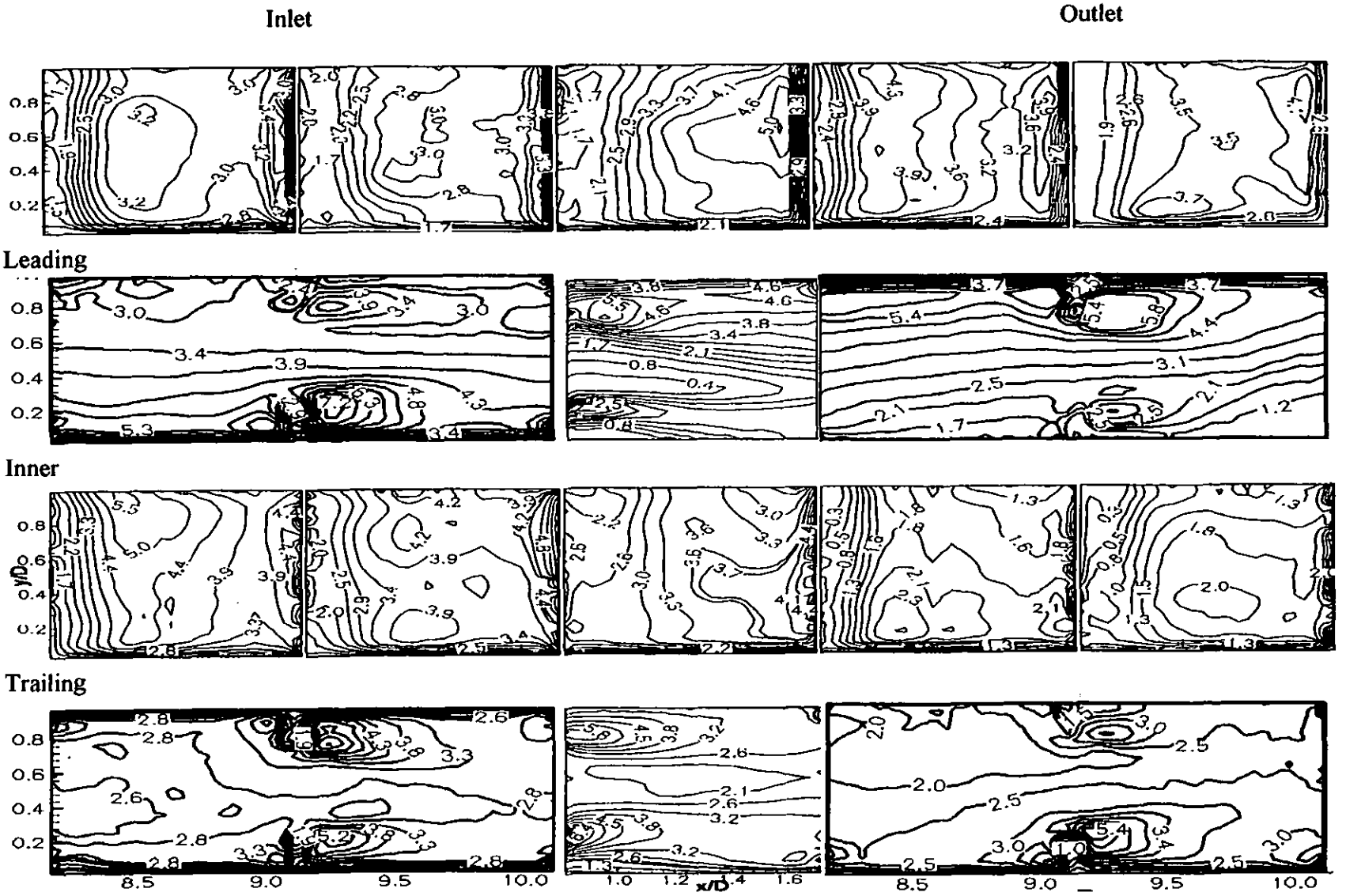

Figure 9: Detailed Sherwood Number Ratio Distributions Sh / Sho in Selected Developing and Fully-Developed Regions for the Ribbed Duct with Horizontal Rod Vortex Generators at Re=30,000, Ro=0.3, s / e=0.55, P / e=10.5, e / D_h=0.1, d / e=0.78.

Downloaded from http://asmedigitalcollection.asme.org/GT/proceedings-pdf/GT1999/78606/V003T01A096/2412441/v003t01a096-99-gt-424.pdf by guest on 28 September 2022

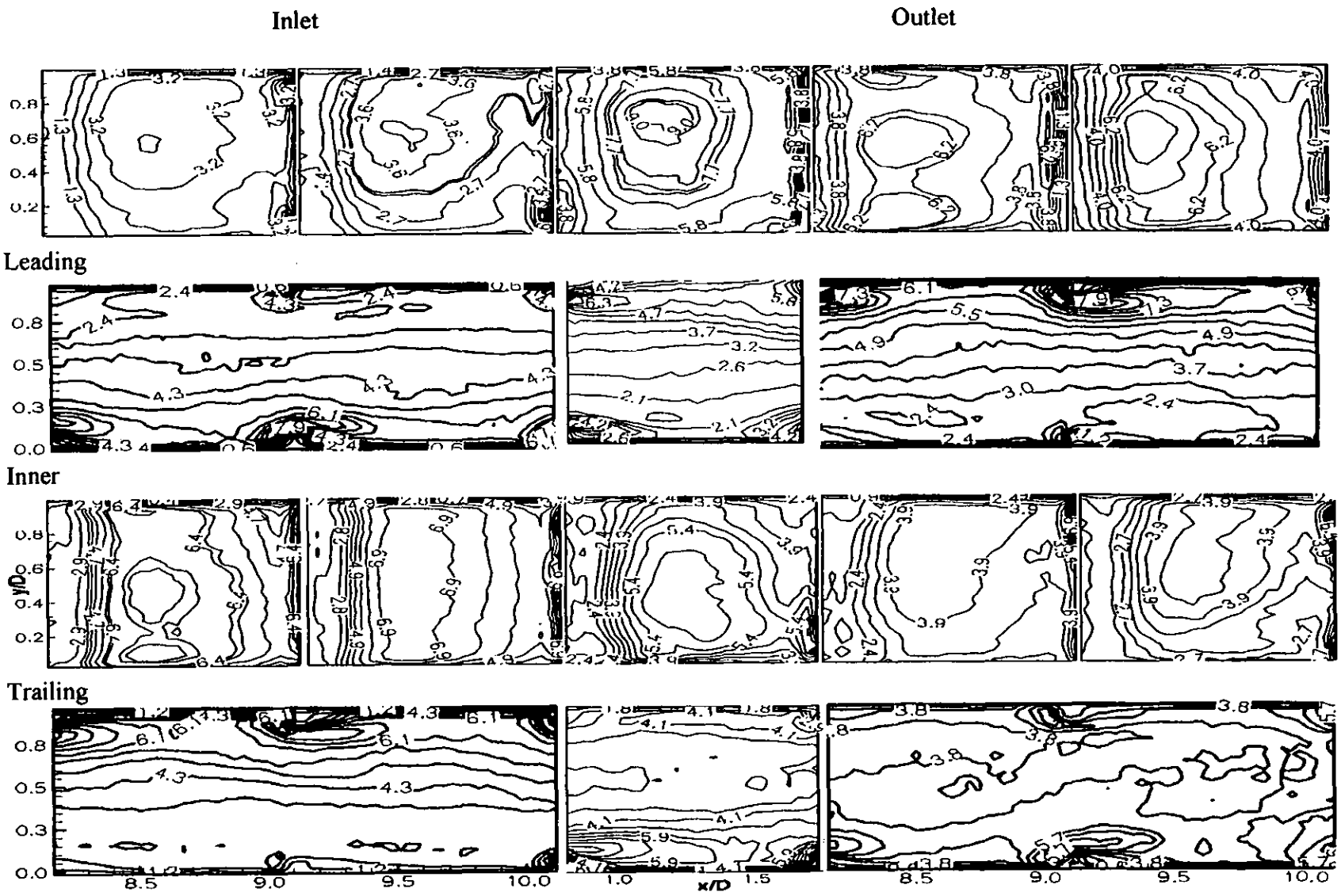

Figure 10: Detailed Sherwood Number Ratio Distributions Sh / Sho in Selected Developing and Fully-Developed Regions for the Ribbed Duct at Re=5,000, Ro=0.3, P / e=10.5, e / D_h=0.1.

Downloaded from http://asmedigitalcollection.asme.org/GT/proceedings-pdf/GT1999/78606/V003T01A096/2412441/v003t01a096-99-gt-424.pdf by guest on 28 September 2022

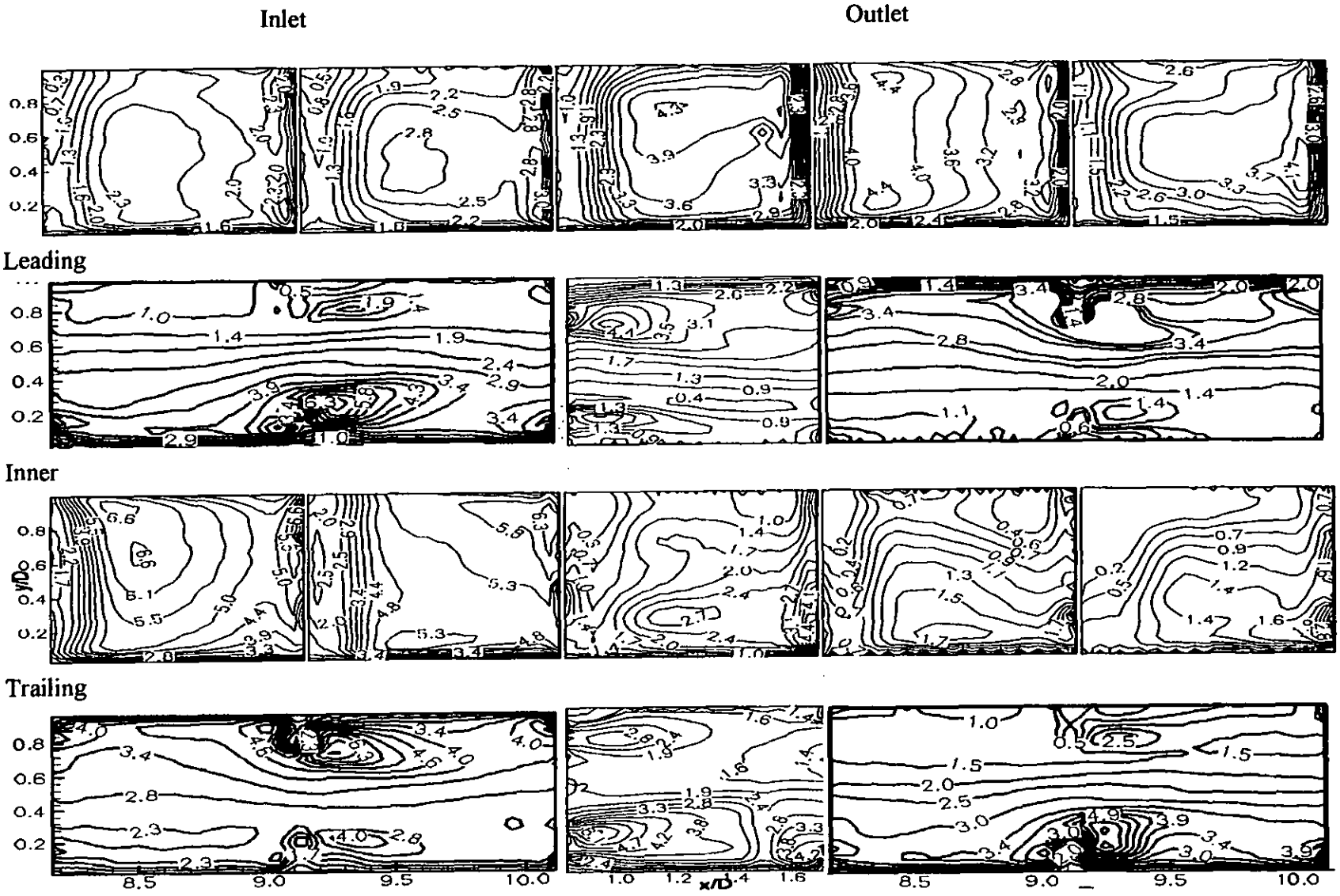

Figure 11: Detailed Sherwood Number Ratio Distributions Sh / Sho in Selected Developing and Fully-Developed Regions for the Ribbed Duct with Horizontal Rod Vortex Generators at Re=5,000, Ro=0.3, s / e=0.55, P / e=10.5, e / D_h=0.1, d / e=0.78.

Downloaded from http://asmedigitalcollection.asme.org/GT/proceedings-pdf/GT1999/78606/V003T01A096/2412441/v003t01a096-99-gt-424.pdf by guest on 28 September 2022